JCTC Journal of Chemical Theory and Computation

Computational Study of the Small Zr(IV) Polynuclear Species

Niny Rao,[†] Marian N. Holerca,[‡] and Vojislava Pophristic*,[†]

Department of Chemistry & Biochemistry and the West Center for Computational Chemistry and Drug Design, University of the Sciences in Philadelphia, Philadelphia, Pennsylvania 19104, and Colgate Palmolive Company, Global Technology Center, Piscataway, New Jersey 08854

Received May 9, 2007

Abstract: Despite widespread zirconium use ranging from nuclear technology to antiperspirants, important aspects of its solvation chemistry, such as the nature of small zirconium(IV) hydroxy cluster ions in aqueous solution, are not known due to the complexity of the zirconium aqueous chemistry. Using a combination of Car−Parrinello molecular dynamics simulations and conventional quantum mechanical calculations, we have determined the structural characteristics and analyzed the aqueous solution dynamics of the two smallest zirconium(IV) cluster species possible, i.e., the dimer and trimer. Our study points to and provides detailed geometrical information for a stable structural motif for building zirconium polymers, the $Zr(OH)_2Zr$ bridging unit with 7−8 coordinated Zr ions, which, however, cannot be used to construct a stable structure for the trimer. We find that a stacked trimer, not featuring this motif, is a possible structure, though not a very stable one, shedding new light on this species, and its possible importance in the aqueous chemistry of Zr^{4+} ion.

I. Introduction

The aqueous chemistry of metal cations is of great interest due to their important roles in chemistry, geochemistry, and biochemistry. The structures, charges, and stabilities of aqueous metal cations and their polynuclear hydrolysis products are crucial for understanding and controlling processes such as their adsorption onto soil/mineral particles; coagulation/precipitation; chemical separations; and interactions with living organisms. Understanding transition and inner transition metal hydrolysis presents a special experimental challenge, due to the complexity and variability of the species formed by these ions in water as well as radioactivity in some cases. Despite decades of research, triggered by applications ranging from drug design to nuclear technology, many physicochemical characteristics of these highly charged ions and their hydrolysis products remain unknown.

The principal experimental problems associated with studying the hydrolysis of highly charged cations are related to the variability and complexity of solution composition and the simultaneous presence of many diverse polynuclear hydrolysis products. Using computational methods, one can isolate a specific chemical species or a combination of species, control the system conditions, and make observations and analyses of processes at the atomic level.

We tackle here the characteristics of polynuclear species formed by solvation of a IVB group metal cation, Zr^{4+}. Our choice of the transition metal to study stems from the important uses of zirconium and the fact that its chemistry is representative of the other IVB group elements as well as our lack of understanding of certain aspects of Zr, Ti, and Hf (group IVB) chemical behavior.[1] For example, Zr^{4+}, Hf^{4+}, and Ti^{4+} polynuclear clusters have been recently found to bind to an Fe^{3+}-binding protein, a member of the transferrin superfamily,[2] which plays a role in biomineralization.[3,4] In addition, Zr^{4+} ion is an essential ingredient of all antiperspirants and thus interacts with human biochemistry through widespread and everyday antiperspirant use, although the

* Corresponding author phone: (215)596-8551; fax: (215)596-5432; e-mail: v.pophri@usip.edu.

[†] University of the Sciences in Philadelphia.

[‡] Colgate Palmolive Company.

10.1021/ct7001094 CCC: $40.75
Published on Web 12/13/2007

nature and the biochemical effect of the specific polynuclear species formed on our skin as a result of Zr^{4+} polymerization are not known.[5]

Most importantly, zirconium metal is a crucial part of zircaloy, the material used in the nuclear fuel rod cladding. Despite its exceptional corrosion resistance, there is an emerging need to model zirconium corrosion due to the long-term possibility that corrosion may lead to leaks of radioactive material, consequent environmental contamination, and ultimately exposure of individuals to radioactivity.[6] The rate of migration of heavy metal ions out of nuclear waste depositories, mining tailings, and coal mines is similarly dependent on the particular hydrolytic species that are present. Common to all the above problems is the need to know exactly what species form in aqueous solutions of these ions under the conditions present and what their physicochemical features are.

In solution, zirconium exists exclusively in a +4 state and is believed to attain coordination numbers of 7 and 8, higher than typical for 3d-transition elements.[7] As opposed to many other transition metals, due to the high charge/radius ratio, Zr^{4+} ion as well as the other two ions of the IVB group (Hf^{4+} and Ti^{4+}) strongly hydrolyzes in water, leading to the formation of polynuclear species with oxygen containing bridges.[7] With few exceptions, neither the structure nor the exact composition of the hydrolyzed mononuclear and polynuclear species have been established. The extent of polymerization depends on many experimental parameters (e.g., aging, temperature, pH, and concentration), resulting in species with very different compositions, often difficult or impossible to distinguish experimentally.[7,8]

Specifically, we present herein our Car−Parrinello molecular dynamics (CPMD)[9] study of the small Zr^{4+} polynuclear cluster species and their behavior in an aqueous environment. The method is uniquely suited to the problem of identifying and analyzing relatively small structures and their behavior in aqueous solutions. This is due to the fact that it does not employ empirically parametrized forces to govern atomic motion but rather determines them "on the fly", along with the molecular dynamics (MD) simulation, from the electronic structure calculations. Thus, CPMD can yield conclusions about interactions between particles in solution as well as properly model important solution processes involving bond breaking and/or formation, such as water deprotonation, and polynuclear species formation and disintegration. The effectiveness of CPMD in ion solvation studies has been demonstrated for a number of cations, including Cu^{2+},[10] Na^{+},[11] Ca^{2+},[12,13] Mg^{2+},[14] Fe^{3+},[15] Y^{3+},[16] K^{+},[17] Al^{3+},[18] Li^{+},[19] and Be^{2+}.[20] CPMD has also been successfully used for identification of unknown structures[21] (including hydrolysis products of ions)[22,23] and studies of their characteristics.[24]

Herein we focus on the two smallest polynuclear species zirconium is thought to form upon dissolution in aqueous media: the dimer and the trimer. Despite the importance of zirconium, only the structure of the tetrameric species ($Zr_4(OH)_8(H_2O)_{16}Cl_8$) is known with certainty, from early X-ray[25,26] and other experiments.[27] X-ray scattering studies have shown that this species is the dominant form in solutions.[26,28]

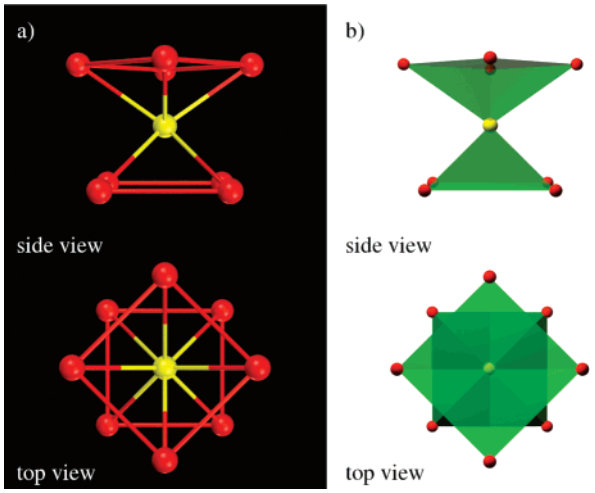

Figure 1. Square antiprism shape used as the building unit for the initial structure design of the dimer and trimer species (see also Figures 2, 3, 6, and 7). Two models (and two views) used further in the text are shown: (a) Ball and stick model - lines represent bonds between Zr^{4+} ion (yellow) and the bridging oxygen atoms (red) and H_2O moieties. (b) Planes cornered by Zr^{4+} ion (yellow) and oxygen atoms (red) represented in solid or translucent colors (green) to facilitate viewing of the structure in space, with perspective.

Spectrophotometric,[29] ultracentrifugation,[30] and light-scattering[31] studies suggest a possible presence of a trimer, $Zr_3(OH)_4^{8+}$, or $Zr_3(OH)_5^{7+}$. However, several recent publications find evidence for only the dimer ($Zr_2(OH)_6^{2+}$ and $Zr_2(OH)_7^{+}$) and tetramer.[1,32] We have determined and characterized the gas-phase and solution structures of the dimer and trimer species using the computational methods described herein and analyzed their stability and chemical behavior in aqueous solution.

II. Methodology

Computational studies of the zirconium system were performed using ab initio (Car−Parrinello) molecular dynamics (CPMD).[9] We employed a Goedecker-type pseudopotential for zirconium[33] and nonlocal norm-conserving soft pseudopotentials of Troullier-Martins type[34] for oxygen and hydrogen. Angular momentum components up to $l_{max} = 2$ have been included for Zr and $l_{max} = 1$ for O. The BLYP exchange correlation functional was employed,[35,36] along with a plane wave basis with a 70 Ry cutoff. All simulations were performed in a periodically repeating cubic box, with the size varying depending on the specific Zr system (see below), with periodic boundary conditions.

Initial structures of the two polymer classes were constructed using a square antiprism as the building unit (Figure 1), based on the expected 7−8 coordination of Zr^{4+} ion, the X-ray structure of the tetramer, and our CPMD simulations of the Zr^{4+} ion in solution.[37] In general, minimum energy geometries of gas-phase structures were obtained by an initial relaxation at 300 K (in some cases 100 and 50 K were used, see section III) for 4−5 ps, followed by simulated annealing and geometry optimization. Simulated annealing runs used scaling factors of 0.9998 and 0.9999 for ionic velocities (unless otherwise noted). The gas-phase simulation cell edge

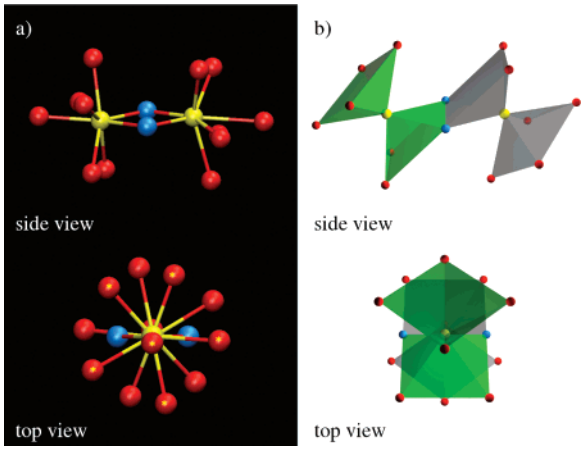

Figure 2. Initial structure of the staggered zirconium dimer. Two Zr^{4+} ions are connected by two O containing bridges and surrounded by additional six H_2O molecules each, in a staggered fashion with respect to the each other. (a) Ball and stick model. Yellow dots in the top view denote oxygen atoms bound to the front zirconium ion. (b) Two square antiprism monomer units are shown in different colors (green, gray) to facilitate viewing. Zr^{4+} ions: yellow; oxygen atoms in the bridging groups: blue; oxygen atoms in H_2O molecules: red. Side and top views are shown. Note that corners (bridge groups and H_2O molecules) of the antiprism units are staggered with respect to each other. Hydrogen atoms are not shown for clarity.

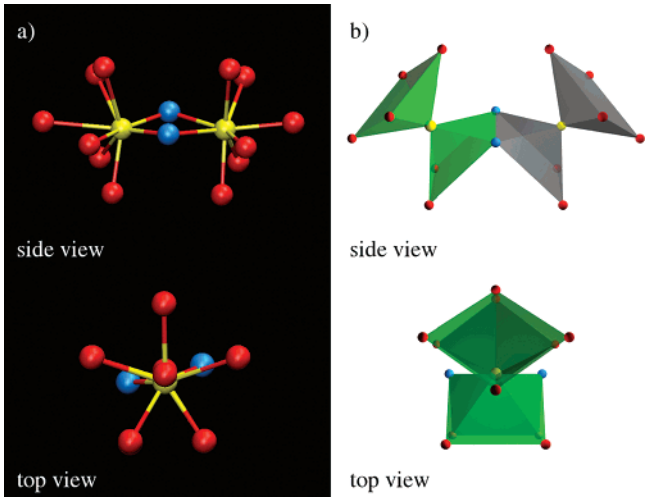

Figure 3. Initial structure of the eclipsed zirconium dimer. Two Zr^{4+} ions are connected by two O containing bridges and surrounded by additional six H_2O molecules each, in an eclipsed fashion with respect to the each other. (a) Ball and stick model. (b) Two square antiprism monomer units are shown in different colors (green, gray) to facilitate viewing. Zr^{4+} ions: yellow; oxygen atoms in the bridging groups: blue; oxygen atoms in H_2O molecules: red. Side and top views are shown. Note that the corners (bridging groups and H_2O molecules) of the antiprism units eclipse each other. Hydrogen atoms are not shown for clarity.

was 12.5 Å for the dimers, 14.0 Å for the compact trimers, and 18.0 Å for the linear trimers. In all calculations, classical equations of motion have been integrated with a velocity Verlet algorithm with a time step of 0.1207 fs and a fictitious mass for the electronic degrees of freedom of $\mu = 500$ au.

After optimization by the CPMD code, structures of the dimer and trimer species were refined by BLYP[38,39] and B3LYP optimizations,[39,40] using the LanL2DZ basis set.[41] These optimizations were carried out by Gaussian03.[42] Harmonic frequencies for the optimized geometries of these species have been calculated to ensure that they correspond to the local minima. The size of the polynuclear species prevented higher level optimizations.

Optimized gas-phase structures were used as the starting geometries for the simulations in aqueous solution. Such computations were undertaken for one dimer species (cubic box with a 12.5 Å edge and 49 H_2O molecules) and one form of the trimer (cubic box with a 15.6 Å edge and 77 H_2O molecules; for the exact form, see section III.B). Stabilities of these species in solution were determined by equilibrating the systems at 300 K using a Nosé-Hoover chain thermostat (of length 4, with frequency 500 cm^{-1})[43−46] for 10 ps.

III. Results

A. Dimer Clusters. The structure of the dimer, constructed as the starting point for the study, consists of two square antiprism units, with corners occupied by H_2O molecules and Zr ions in the centers of the units; these units are connected by two O containing bridges, with no direct Zr−Zr bond (Figure 2). Water molecules were chosen for the ligands following the structure of Zr^{4+} tetramer, which is the only Zr polynuclear species whose structure has been obtained both experimentally (e.g., X-ray studies) and by computational means ($Zr_2(OH)_6^{2+}$ and $Zr_2(OH)_7^{+}$, observed experimentally, form in solutions with pH<3.5). Several variants of the general dimer structure with respect to the bridge composition were subjected to the CPMD simulation in gas phase at 300 K. We tested the following structures: (a) a dimer with two OH bridges $[Zr_2(OH)_2(H_2O)_{12}^{6+}]$; (b) a dimer with an O and an OH bridge $[Zr_2O(OH)(H_2O)_{12}^{5+}]$; (c) a dimer with an H_2O and an OH bridge $[Zr_2(H_2O)(OH)(H_2O)_{12}^{7+}]$; and (d) a dimer with two O bridges $[Zr_2(O)_2(H_2O)_{12}^{4+}]$. The structure described under (c) proved to be unstable, as the H_2O bridge departed the cluster in the course of the gas-phase CPMD simulation (we observe the following reaction: $[Zr_2(H_2O)(OH)(H_2O)_{12}^{7+}] \rightarrow [(H_2O)_5Zr\text{-}(OH)\text{-}Zr(H_2O)_5^{7+}] + 3H_2O$). In the other three cases, the dimer structures persist for about 3 ps (length of the simulation), in the staggered conformation as described below for the $[Zr_2(OH)_2(H_2O)_{12}^{6+}]$ cluster. Due to the computational expense associated with CPMD simulations, we focused on only one structure for further investigations. The $[Zr_2(OH)_2(H_2O)_{12}^{6+}]$ cluster was chosen based on its similarity to the Zr tetramer structure.[47]

For the $[Zr_2(OH)_2(H_2O)_{12}^{6+}]$ cluster, two initial conformations have been constructed (Figures 2 and 3). The first conformation, which will be referred to as the *staggered* conformation, has H_2O molecules which coordinate the two Zr^{4+} ions, 36° out of phase with each other (Figure 2). In the second conformation, the H_2O molecules surrounding two Zr^{4+} ions overlap each other (Figure 3), so this form is referred to as the *eclipsed* conformation. Both structures were

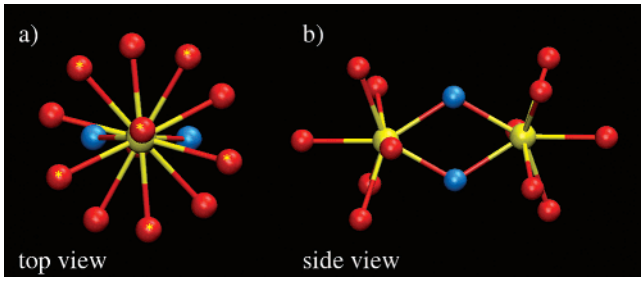

Figure 4. Optimized structure of the $[Zr_2(OH)_2(H_2O)_{12}{}^{6+}]$ dimer (BLYP/plane wave optimized structure shown; general features are the same as in the B3LYP/LanL2DZ and BLYP/LanL2DZ optimized ones; for the differences, see Table 1). Views shown: (a) view along the Zr−Zr axis. Only bonds connecting Zr^{4+} ions and oxygen atoms are shown. Yellow stars in the top view denote oxygen atoms bound to the front zirconium ion. (b) Side view, showing the plane consisting of two Zr^{4+} ions and two OH bridges. Zr^{4+} ions: yellow; oxygen atoms in OH bridging groups: blue; oxygen atoms in H_2O molecules: red.

subjected to relaxation at 300 K followed by simulated annealing in gas phase. During the relaxation phase (5 ps), the eclipsed conformation converted to the staggered conformation and remained stable throughout the simulated annealing. The staggered conformation, as expected, did not change its general features in the course of this procedure. Simulated annealing started from either the staggered or the eclipsed forms resulted in the same optimized structure, shown in Figure 4. These results indicate that the stable conformation of the dimer is the staggered one, as a consequence of a better accommodation of the steric crowding.

The annealed structure was optimized using plane wave basis, yielding a roughly symmetrical final conformation, with a Zr−Zr distance of 3.8 Å (Figure 4, Table 1). The two oxygen atoms in OH bridges are 2.2 Å apart from each of the zirconium ions. Oxygen atoms at the corners of the pyramid bases of the two units are staggered with respect to each other when viewed along the Zr−Zr axis. More precisely, oxygen atoms at the corners of the top monomer are 36° out of phase from those in the bottom monomer (Figure 4). The structure was also subjected to optimization using BLYP and the B3LYP/LanL2DZ level, with results in close agreement to the ones described above (Table 1). The obtained distance between Zr atoms and bridging O atoms is in the range of the values published for related Zr compounds in the solid state, such as the tetragonal (both experimental and calculated) ZrO_2 structure (2.09−2.44 Å)[48] and the calculated amorphous ZrO_2 (2.04−2.25 Å).[49] The Zr−Zr distance is, as expected, somewhat larger than in the monoclinic ZrO_2 structure (crystal structure data), which is 3.44−3.47 Å.[50] Our values also agree with the calculated gas-phase Zr−O bond lengths in a series of $Zr(OH)_n(H_2O)_m$ monomers with varying n, m ($Zr-O_{OH}$: 1.9−2.2 Å; $Zr-O_{H2O}$: 2.2−2.4 Å).[51]

In order to explore the dimer structure in aqueous solution, the optimized staggered structure was placed in a box with 49 H_2O molecules. The system was allowed to evolve for 10 ps at 300 K using a Nosé-Hoover chain thermostat. Analysis of the final trajectory revealed that both Zr−O radial

Table 1. Geometrical Parameters of the Optimized Zr^{4+} Dimer ($Zr_2(OH)_2(H_2O)_{12}{}^{6+}$), Obtained Using Different Computational Levels[a]

	BLYP/plane wave basis	BLYP/ LanL2DZ	B3LYP/ LanL2DZ
	Distance (Å)		
Zr−Zr	3.751	3.871	3.819
$Zr-O_{OH}$	2.195−2.218	2.251−2.255	2.226−2.227
$Zr-O_{H2O}$	2.268−2.356	2.270−2.363	2.249−2.334
	Angle (deg)		
$O_{OH}-Zr-O_{OH}$	63.39−63.48	61.55	61.94
$Zr-O_{OH}-Zr$	116.44−116.69	118.44−118.46	118.06
$O_{OH}-Zr-O_{H2O}$ (1)[b]	75.80−91.07	77.27−94.57	77.17−94.53
$O_{OH}-Zr-O_{H2O}$ (2)[c]	79.48−79.70	79.86−81.99	79.78−81.98
$O_{H2O}-Zr-O_{H2O}$ (1)[d]	71.47−71.52	71.93−71.94	71.89−71.92
$O_{H2O}-Zr-O_{H2O}$ (2)[e]	71.71−81.16	71.33−79.18	71.30−79.07
$O_{H2O}-Zr-O_{H2O}$ (3)[f]	70.30−73.97	69.68−73.27	69.76−73.29

[a] The optimized Zr dimer has a staggered configuration, in which two antiprism units are joined along the edge defined by the two OH bridges. The pyramids that contain this OH−OH edge are defined as base pyramids; the other two pyramids are defined as top pyramids. [b] $O_{OH}-Zr-O_{H2O}$ (1) refers to angles defined by hydroxyl O, Zr, and water O atoms in the top pyramids. [c] $O_{OH}-Zr-O_{H2O}$ (2) refers to angles defined by hydroxyl O, Zr, and water O atoms in the base pyramids. [d] $O_{H2O}-Zr-O_{H2O}$ (1) refers to angles defined by water O atom in the base pyramids, Zr, and the other water O atoms in the same base pyramid. [e] $O_{H2O}-Zr-O_{H2O}$ (2) refers to angles defined by water O atoms in the base pyramids, Zr, and water O atoms in the top pyramids. [f] $O_{H2O}-Zr-O_{H2O}$ (3) refers to angles defined by water O atoms in the top pyramids, Zr, and water O atoms in the same top pyramid.

distribution functions (for the two Zr^{4+} ions) have peaks at ∼2.2 Å, whereas the corresponding number of integrals show plateaus at 7 and 8, indicating different coordination numbers for the two Zr^{4+} ions (Figure 5a). Further examination of the trajectory revealed that one of the zirconium ions loses one of the initially eight coordinating water molecules within the first 1 ps of the simulation. We also note that the water molecules bound to the complex do not exchange with the bulk water molecules on the time scale of the simulation, as evident from the flat and long plateau of the radial distribution function (g(r)) at the zero value between the peaks for the first and the second shell of coordinated water (2.7−3.7 Å, Figure 5a). The Zr−Zr distance oscillates around 3.65 Å, with no drift (Figure 5b), indicating the general stability of the cluster. The first shell water molecules are organized around each zirconium ion in a pyramidal fashion (Figure 5c), the overall final arrangement being similar to that of the gas phase, except for one pyramid that lacks a water molecule. More specifically, the geometry of the first coordination shell of the eight-coordinated Zr ion corresponds to an antiprism, with the peaks of the angular distribution function (the plotted angle is ∠O−Zr−O) coinciding with those of the ideal antiprism (70°, 82°, 108°, and 142°). The peak at 70−85° (corresponding to the 70° and 82° peaks of the ideal antiprism) stems from two kinds of O−Zr−O angles: ∠O−Zr−O formed by the oxygen atoms which are next to each other and are located within the same pyramid (ideally 70°), and ∠O−Zr−O in which one oxygen atom is from the top and the other one is from bottom pyramid, and which are 45° out of phase from each other (ideally 82°). Another peak is centered at 140°, and is produced by the

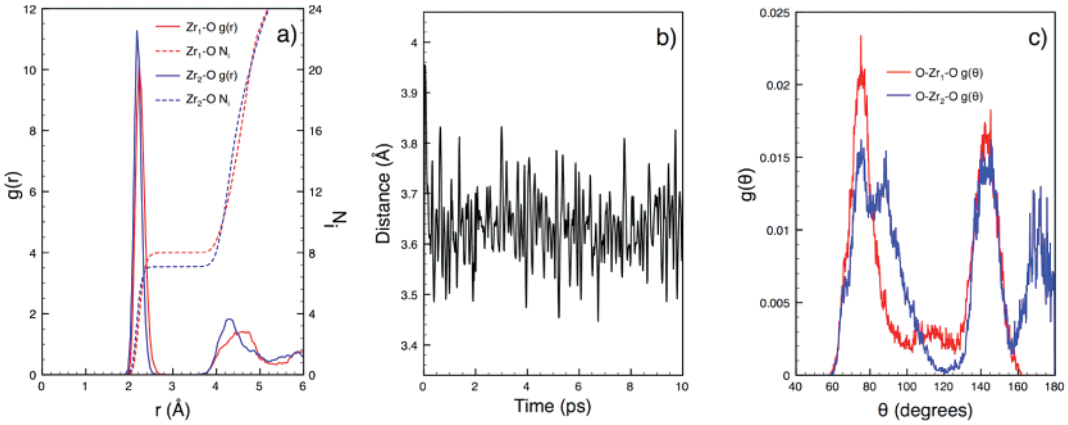

Figure 5. Zirconium dimer ($Zr_2(OH)_2(H_2O)_{12}^{6+}$) in solution. (a) The Zr−O radial distribution functions (g(r), solid lines) and corresponding running coordination number integrals (NI, dashed lines) for the two Zr^{4+} ions. Note the difference between the coordination numbers for the two Zr^{4+} ions (7 and 8). (b) Zr−Zr distance as a function of time. (c) Angular distribution function. Angle plotted: ∠O−Zr−O. Arrangement of H_2O and OH groups around the eight-coordinated Zr ion (red) corresponds to an antiprism, whereas this arrangement around the seven-coordinated Zr ion (blue) corresponds to a pentagonal bipyramid.

O−Zr−O angle defined by oxygen atoms from the top and bottom pyramids, 135° out of phase from each other (ideally 142°). A much less pronounced feature at 105−115° comes from the O−Zr−O angle in which both oxygen atoms are located within the same pyramid and are opposite to each other (ideally 108°). The angular distribution function of the seven-coordinated Zr ion is clearly distinct from the eight-coordinated Zr case and indicates a pentagonal bipyramid geometry. Its coordinating groups produce peaks at 75° (angle between O atoms in the pentagonal base), 90° (angle between O atoms in pyramid plane and pyramid corner), 140° (angle between second nearest neighbors in the pentagonal base), and 180° (angle between two pyramid apexes), coinciding with the ideal pentagonal bipyramid peaks at 72°, 90°, 144°, and 180°. In both cases, departures from the ideal peak positions and widths are due to thermal fluctuations as well as the bending imposed by the existence of the two OH bridges.

Although data for direct comparison with experimental values are not available, the Zr−Zr and Zr−O distances fall within the range of values observed in dinuclear zirconium organometallic complexes, such as the one with the heptadentate ligand dhpta (reported average Zr−Zr and Zr−O distances are 3.5973 Å and 2.165 Å, respectively)[52] and the one with lactate ligands (3.5 Å and 2.0−2.2 Å, respectively).[53]

In summary, we find that a dimer structure with two OH bridges and 5−6 water molecules coordinating Zr^{4+} ions is stable both in gas-phase and aqueous solution, on the time scale of our simulation. The major difference between the gas-phase and aqueous solution results is in that the aqueous structure has one seven-coordinated and one eight-coordinated Zr^{4+} ion, as opposed to the two eight-coordinated Zr ions in gas phase. The arrangement of the terminal water molecules and OH groups within the monomer units is either square antiprism or pentagonal bipyramid, depending on the coordination, and the spatial relationship between the two units is such that water molecules are staggered.

B. Trimer Clusters. With an increasing number of Zr^{4+} ions, possibilities for different arrangements of the monomer units increase rapidly. Although more trimer configurations are conceivable, we focus here on two general configurations: linear and stacked (Figures 6 and 7). The linear structure consists of three antiprism units connected by bridges (Figure 6); the more compact, stacked structure consists of three monomer units joined by three bridges, each shared by two adjacent Zr^{4+} ions, and one, central bridge which is shared by all three Zr^{4+} ions (Figure 7). We attempted several compact trimer structures with respect to the nature of the bridges (the H_2O bridges were not considered based on the dimer result described in the previous section): (a) all four bridges are O^{2-} ions; (b) all four bridges are OH groups; (c) the central bridge, shared by three Zr^{4+}

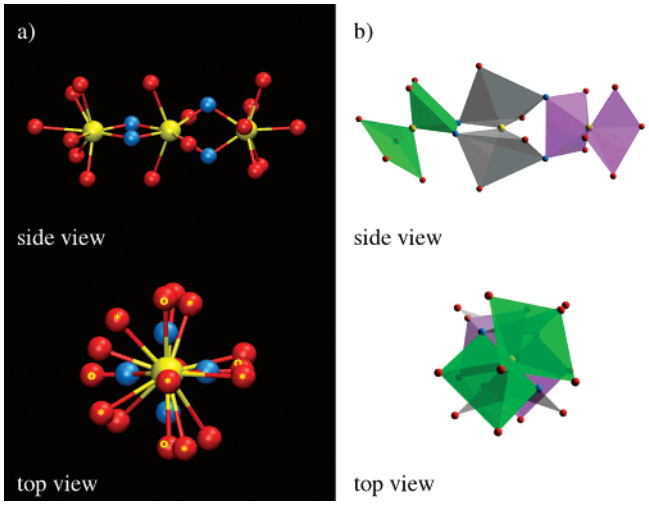

Figure 6. Initial structure of the linear trimer ($[Zr_3(OH)_4(H_2O)_{16}]^{8+}$). Three Zr^{4+} ions are connected by four OH bridges, in a linear fashion. (a) Ball and stick model. Yellow stars in the top view denote oxygen atoms bound to the front zirconium ion, whereas open yellow circles denote oxygen atoms bound to the middle Zr^{4+} ion. (b) Three square antiprism monomer units are shown in different colors (green, gray, purple) to facilitate viewing. Zr^{4+} ions: yellow; oxygen atoms in OH bridging groups: blue; oxygen atoms in H_2O molecules: red. Side and top views are shown.

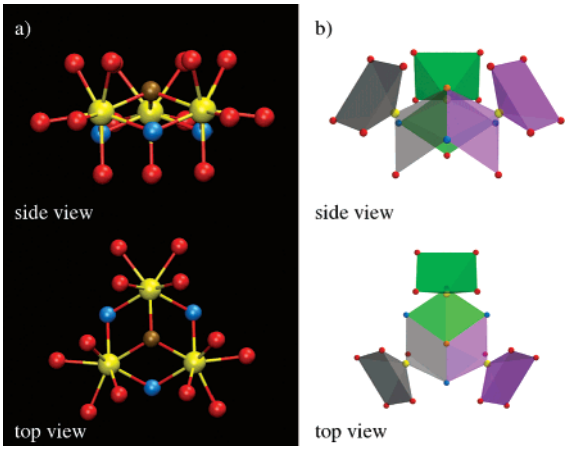

Figure 7. Initial structure of the stacked trimer. Three Zr^{4+} ions are connected by three bridges, and share another bridging group through a second set of three bridges. (a) Ball and stick model. (b) Three square antiprism monomer units are shown in different colors (green, gray, purple) to facilitate viewing. Zr^{4+} ions: yellow; oxygen atoms in bridging groups shared by two Zr^{4+} ions each: blue; oxygen atom bound to all three Zr^{4+} ions: brown; oxygen atoms in H_2O molecules: red. Side and top views are shown.

ions, is an OH group (brown, Figure 7); the three bridges, shared by two Zr^{4+} ions each (blue, Figure 7), are O^{2-} ions; (d) the central bridge is an O^{2-} ion, and two out of three bridges shared by two Zr^{4+} ions each are OH groups, with the remaining bridge an O^{2-} ion; (e) the central bridge is an O^{2-} ion, and two out of three bridges shared by two Zr^{4+} ions each are O^{2-} ions, with the remaining bridge an OH group; and (f) the central bridge is an O^{2-} ion, and the three bridges shared by two Zr^{4+} ions each are OH groups.

The initial configuration of the linear trimer was constructed by placing three Zr monomer units next to each other so that the two sets of OH bridges (connecting the first and the second unit, and connecting the second and the third unit) are 90° out of phase with respect to each other to minimize steric crowding effects. The Zr−Zr−Zr angle was set to 180°. Each Zr^{4+} ion was surrounded by water molecules (six and four for the terminal and middle Zr^{4+} ions, respectively) so that the coordination of eight was achieved. In addition, a bent linear structure was studied in which the Zr−Zr−Zr angle was set to 132°.

The stacked trimer was constructed by arranging each of the monomer units around three adjacent faces of a cube. The joint vertex of these three faces of the cube is occupied by the bridging group shared by three Zr^{4+} ions, while the bridges that connect two Zr^{4+} ions each occupy the remaining vertices (Figure 7). The Zr ions are placed above the center of each face, and additional water molecules are added so that each monomer unit is eight coordinated in an antiprism configuration. The zirconium ions are placed at an equal distance of 3.76 Å from each other. Intuitively, the stacked structure (shown in Figure 7) should be more stable than the linear one, due to its more compact geometry and additional linking bridges with respect to the linear trimer (6 bridges in the stacked trimer vs 4 bridges in the linear one). Such a stability order was also observed in a computational study of Al^{3+} cluster species.[54]

We first attempted to obtain a stable trimer structure in a fashion similar to the one used for the dimer: the described initial configurations were allowed to relax at 300 K in the gas phase. In the course of the gas-phase CPMD simulation at 300 K, with the exception of the above-described structure (b), which completely falls apart, all attempted stacked trimers follow a similar behavior, in that two Zr^{4+} ions remain at the distance of 3.0−3.2 Å, throughout the 7 ps simulation time, whereas one Zr^{4+} ion moves to a longer distances of 3.6−4.0 Å from the other two ions, extending the related bridges. Due to the computational cost of CPMD simulations (especially in aqueous solutions), we have chosen one of the above-described structures ($[Zr_3(OH)_3O(H_2O)_{18}]^{7+}$) to extensively investigate with respect to both the gas-phase and aqueous solution dynamics (the choice is based on the structural relationship to the Zr^{4+} hexamer[55]). As we will discuss later in the text, on the CPMD accessible time scale, the trimer species exhibit a "breathing" behavior, in which the Zr^{4+} ion which initially moves somewhat away from the other two Zr^{4+} ions periodically comes back forming roughly the initial stacked trimer structure.

In an attempt to further examine the stability of the stacked trimer with respect to the Zr^{4+} ion drifting away from the cluster, the simulation for $[Zr_3(OH)_3O(H_2O)_{18}]^{7+}$ was repeated at 100 K and at 50 K, neither of which was able to capture the anticipated degree of stability (i.e., no drifting of the Zr^{4+} ion). We also used the following procedure: all of the distances between Zr ions and O atoms were constrained to 2.3 Å, whereas O−H bonds as well as the corresponding bond angles and dihedral angles were permitted to change in the course of the simulation. Thus the water molecules around each Zr ion were allowed to relax to their optimal positions, while the monomer units were forced to remain bound to each other. The constrained CPMD simulation was carried out for 5 ps at 300 K and was followed by unconstrained simulated annealing using a scaling factor of 0.999. The stacked trimer remained mostly intact with only a H_3O^+ moiety leaving the main cluster. The geometrical/structural changes that occurred during the gas-phase simulation are described below.

With respect to the linear trimer, a "straight" and a "bent" form were tested. Both forms fall apart in the initial stages of CPMD gas-phase simulation. We attempted the constrained CPMD simulation as described for the stacked trimer, but, in the course of simulated annealing, the trimers disintegrated by the cleavage into a monomer and a dimer occurring at the OH bridges (resulting in one OH group leaving with the monomer unit and the other one remaining with the dimer). The geometry of the dimer is similar to the one described in section III.A. In conclusion, no stable linear trimer was observed.

The stacked trimer obtained from the constrained CPMD followed by simulated annealing had the following properties. The final configuration retained roughly its equilateral triangular shape, with Zr−Zr distances of 3.60, 3.54, and 3.51 Å. However, two of the zirconium ions have the coordination number of 7, while the third zirconium ion has

Table 2. Optimized Geometry of the $[Zr_3(OH)_3O(H_2O)_{18}]^{7+}$ Trimer, Obtained Using Different Computational Levels[a]

	BLYP/plane wave basis	BLYP/ LanL2DZ	B3LYP/ LanL2DZ
	Distance (Å)		
Zr−Zr	3.487−3.604	3.588−3.607	3.553−3.572
$Zr-O_{OH}$	1.903−2.221	1.914−2.318	1.901−2.296
$Zr-O_{bridge}$	2.074−2.291	2.065−2.193	2.149−2.167
$Zr-O_{H2O}$	2.193−2.368	2.241−2.356	2.224−2.327
	Angle (deg)		
Zr−Zr−Zr	57.97−61.20	59.75−60.26	59.74−60.28
$O_{OH}-Zr-O_{OH}$	106.56−111.67	100.18−113.94	106.90−108.64
$Zr-O^{2-}-Zr$	110.54−114.33	111.38−115.67	111.70−115.72
O−Zr−O[b]	65.98−85.14	65.28−91.29	65.42−90.94
O−Zr−O[c]	106.29−162.91	100.18−172.05	100.86−171.50
O−Zr−O[d]	74.63−133.83	71.24−134.17	71.61−134.26
O−Zr−O[e]	146.59−152.79	147.05−151.63	147.12−151.86

[a] See text for the discussion about differences between the optimized structures. [b] O−Zr−O refers to angles defined by O, Zr, and O atoms in which the Zr and O atoms lay on the pentagonal base, and O atoms are adjacent to each other. The value for such an angle in an ideal pentagonal bipyramid is 72°. [c] O−Zr−O refers to angles defined by O, Zr, and O atoms in which the Zr and O atoms lay on the pentagonal base, and O atoms are not adjacent to each other. The value for such an angle in an ideal pentagonal bipyramid is 144°. [d] O−Zr−O refers to angles defined by an O atom located on the pentagonal base, and Zr and O atoms are located below or above the pentagonal base. The value for such an angle in an ideal pentagonal bipyramid is 90°. [e] O−Zr−O refers to angles defined by an O atom located below the pentagonal base, a Zr atom within the base, and an O atom located above the base. The value for such an angle in an ideal pentagonal bipyramid is 180°.

a final coordination number of 8. During the simulated annealing, one of the water molecules initially surrounding a Zr ion moved away from the first coordination shell, settling at the distance of 10.64 Å from the Zr^{4+} ion it originated from, while abducting a proton from a water molecule remaining within the cluster (bound to the same Zr ion). Subsequently, a second water molecule broke away from another Zr^{4+} ion and reached a stable distance of 4.5 Å from the Zr^{4+} ion it was bound to and that same distance to the eight-coordinated Zr^{4+} ion. Thus, the resulting cluster has two seven-coordinated Zr ions, one of which has a terminal OH group instead of a H_2O molecule.

The annealed structure was subjected to optimization at the B3LYP/LanL2DZ level, with the resulting geometrical parameters summarized in Table 2 (also see Figure 8). During the B3LYP optimization, one H_3O^+ moiety moved away from the cluster, resulting in a stacked trimer with three seven-coordinated Zr units. In other words, in addition to the two OH^- and one O^{2-} bridges, two of the three Zr ions have one OH group and three water molecules in the coordination shell. This structure was confirmed by BLYP/LanL2DZ optimization (Table 2). The BLYP/plane wave optimization was conducted starting from the geometry taken at the 10th ps of the CPMD simulation following the simulated annealing (discussed in the next paragraph). The difference with respect to the B3LYP/LanL2DZ geometry is that only one Zr ion has a coordination shell with an OH group. Other geometrical parameters are in agreement with the two other reported levels (Table 2). All Zr ions in the three optimized structures have a distorted pentagonal bipyramid configuration, with a range of values for the angles, centered at the value of the ideal pentagonal bipyramid (see footnote, Table 2). Further comparison with literature data is not possible, since the literature information is scarce and conflicting: no structure description has been published, and several compositions have been suggested and disputed.[1,56,57]

To determine the stability of the observed structure, the stacked trimer obtained from the simulated annealing process described above was simulated further. After a 5 ps gas-phase equilibration at 300 K using a Nosé-Hoover chain thermostat, the system was allowed to evolve for 50 ps. During the 50 ps CPMD simulation, a third water molecule (in addition to the two water molecules which left the cluster during simulated annealing) moved away from the first coordination shell of the remaining eight-coordinated Zr ion, to a distance of 4.15 Å from the nearest Zr^{4+} ion, making all three Zr^{4+} ions seven-coordinated, the same as that obtained by geometry optimizations (Figure 9a). The remaining bound water molecules produce a sharp g(r) peak at 2.2 Å distance for each of Zr^{4+} ions, with the running coordination number plateaus clearly at seven. In the case of the Zr^{4+} ion which has a terminal OH group in its first coordination shell, we observe two peaks in the radial distribution function: one at 1.8 Å, corresponding to the oxygen atom of the terminal (not a bridging one) OH group, and another one at 2.2 Å, stemming from oxygen atoms of terminal water molecules. Also, after the initial 11 ps of the simulation, the Zr^{4+} ion unit with one terminal OH^- group started drifting away from the cluster. It settled at a distance of ∼4.1 Å from the other two Zr^{4+} ions. This configuration persisted for about 6 ps, when the Zr^{4+} ion unit drifted back to ∼3.6 Å from the other two Zr^{4+} ions, and remained in this configuration for about 2 ps, followed by another movement to ∼4.1 Å from the other Zr^{4+} ions, where it again remained for ∼5 ps. After coming close to the rest of the cluster (remaining there for ∼4 ps), this unit departed the cluster again, this time remaining at ∼4.1 Å for ∼15 ps (Figure 9b), afterward joining the cluster for >6 ps. Thus, we observe an irregular oscillatory movement of one Zr unit with respect to the other two. At each instance of this Zr^{4+} ion moving away, the two other Zr^{4+} ions come closer to each other with respect to their distance in the initial several picoseconds of the simulation, as a consequence of decreased steric crowding. Moreover, the central bridging oxygen atom was observed to move above and below the plane defined by the three Zr^{4+} ions (Figure 9c) during the first 10 ps of simulation. From this point onward, this oxygen atom was found to remain on one side of the plane defined by the three Zr^{4+} ions. Thus, at all the times, one atom or a group of atoms was moving away from the rest of the cluster: in the first 10 ps, it was the central, bridging O atom; afterward, it was a Zr monomer unit.

The stacked trimer structure was then tested in solution, by placing the structure obtained at the end of the gas-phase constrained dynamics run in a box with 73 water molecules (15.6 Å size) and simulating the system for 10 ps. We find that all three Zr ions remain seven-coordinated (Figure 10a), with oxygen atoms of the coordinating species at 2.2 Å from

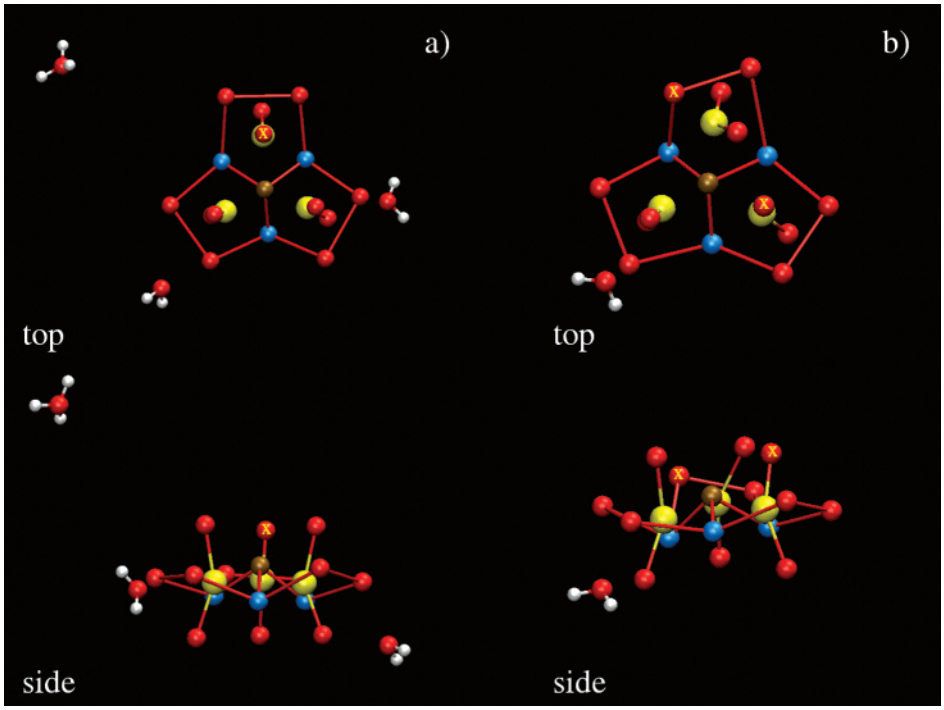

Figure 8. Optimized structure of the stacked trimer ($[Zr_3(OH)_3O(H_2O)_{18}]^{7+}$). (a) Structure optimized by BLYP/plane wave basis set. (b) Structure optimized using the B3LYP/LanL2DZ basis set. The connecting lines show the pentagonal base in the pentagonal bipyramid arrangement of each Zr unit (not the chemical bonds). The Zr^{4+} ions are located at the center of each base. The axial oxygen atoms are connected to the Zr ions to show their axial position with respect to the pentagonal base. Zr^{4+} ions: yellow; oxygen atoms in OH bridging groups: blue; oxygen atom bound to all three Zr^{4+} ions: brown; oxygen atoms in H_2O molecules: red. The oxygen atoms in terminal OH groups are marked by a yellow "x" sign. Side and top views are shown.

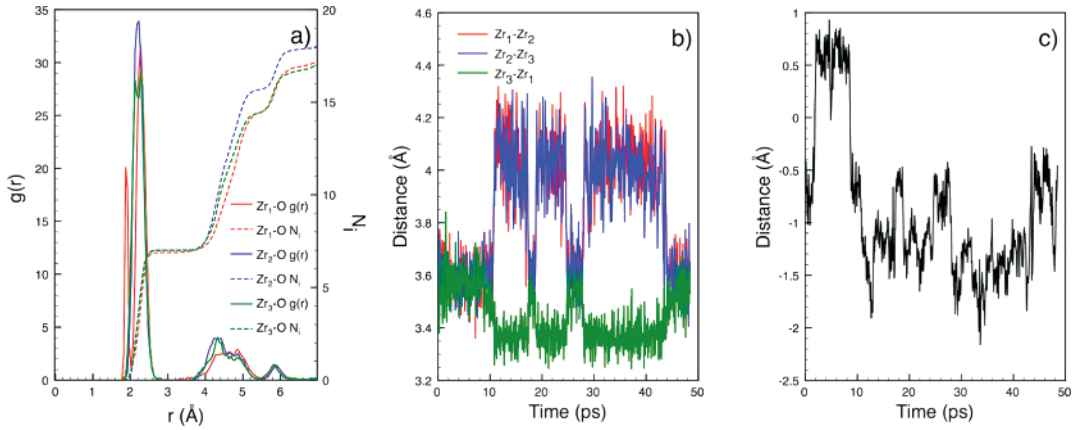

Figure 9. CPMD simulation of the stacked trimer ($[Zr_3(OH)_3O(H_2O)_{18}]^{7+}$) in gas phase. (a) Zr−O radial distribution function (g(r), solid line) and the corresponding running integral coordination numbers (NI, dashed line) for the three Zr^{4+} ions. (b) Zr−Zr distance for all three possible pairs of Zr^{4+} ions (red, blue, and green lines). Note that one of the Zr^{4+} ions (red, blue) moves ∼4.2 Å away from the other two in the 11th, 19th, and 28th ps of the simulation and remains at that distance for ∼7 and ∼16 ps. As this happens, the distance between the other two Zr^{4+} ions shrinks slightly, as a consequence of decreased steric crowding. (c) Distance of the O atom shared by the three Zr ions from the plane defined by the three Zr ions. The change of sign from positive to negative indicates that the O atom is moving from one side of the plane to the other.

the Zr ion. On the scale of the simulation, no exchange between the terminal and bulk water molecules is observed. Figure 10b illustrates the stability of the cluster within the 10 ps simulation time—the Zr−Zr distances oscillate around 3.54 Å, with no drift. The spatial arrangement of the coordinating species (one O bridge, two OH bridges, and four H_2O molecules) of the three seven-coordinated Zr ions is somewhat different from the dimer seven-coordinated unit: the locations of the peaks of the angular distribution functions point to a significantly distorted pentagonal bipyramid (Figure 10d). The ∼72° peak, characteristic of the pentagonal bipyramid (angle between the species on the pentagonal base) is present. The main distortion from the ideal pentagonal bipyramid occurs with the position of the oxygen atoms perpendicular to the pentagonal base (axial oxygen atoms); instead of a 90° angle with the base, we

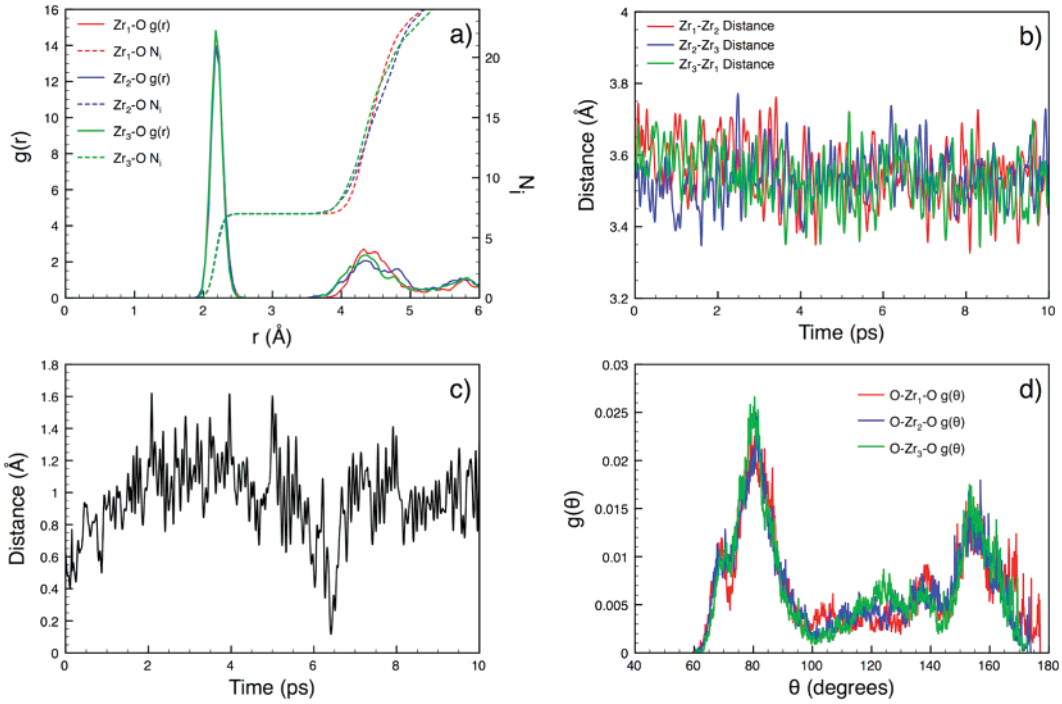

Figure 10. CPMD simulation of the stacked trimer ($[Zr_3(OH)_3O(H_2O)_{18}]^{7+}$) in aqueous solution. (a) The Zr−O radial distribution functions (g(r), solid lines) and corresponding running coordination number integrals (NI, dashed lines) for the three Zr^{4+} ions, indicating their seven coordination. (b) Zr−Zr distance for the three pairs of the Zr ions, oscillating around 3.54 Å. (c) Distance of the O atom shared by the three Zr ions from the plane defined by the three Zr ions. Unlike the gas-phase simulation, the O atom did not move from one side of the plane to the other. (d) Angular distribution function for the three Zr ions (O−Zr−O angle plotted), indicating a distorted pentagonal bipyramid arrangement of the coordinating oxygen atoms around each of the Zr ions.

observe an 85° angle. In addition, instead of an ideal linear arrangement (180°) between the two axial oxygen atoms around the same Zr ion, we find a peak at 155°.

In summary, we find that the stacked trimer is a possible, but not very stable, structure in the gas phase. A notable dynamical feature of the gas-phase structure is the oscillation of one monomer unit (shown here through the motion of the corresponding Zr^{4+} ion, Figure 9b), which might ultimately lead to cluster disintegration on a longer time scale. However, CPMD simulations beyond ∼50 ps presented here are not practical at this point in time. This motion was not observed in the course of the simulation in aqueous solution, due to the shorter simulation time as well as constraints posed by water molecules that surround the cluster (longer simulation, impractical at this time, is predicted to show one monomer unit leaving the cluster as well). In the course of the 10 ps simulation in solution, the species appears stable, with Zr−Zr distances oscillating around 3.54 Å. All three Zr ions remain surrounded by seven ligands (a bridging O group, two bridging OH groups, and four H_2O molecules; unlike the gas-phase structure, no terminal OH groups were found in the first coordination shell), arranged in a distorted pentagonal bipyramid geometries.

IV. Discussion

The present CPMD simulations, along with those presented in ref 47 show that several small Zr^{4+} polynuclear clusters exist in aqueous solution as structures consisting of seven- and eight-coordinated monomer units, with common features. Whereas the dimer and the tetramer[47] appear stable at the picosecond time scale, the trimer undergoes internal motions which indicate a possible cluster disintegration at a later stage.

The basic structural motif seen in the studied forms is a seven to eight coordinated Zr^{4+} ion, consistent with the coordination assigned to the Zr^{4+} ion in general.[7] The zirconium ion is surrounded by H_2O molecules and OH (or O^{2-}) groups, with Zr−O bonds of ∼2.2 Å length. After a certain coordination is assumed in the course of gas-phase structure determination, the initial changes in the coordination shells and settling to a certain coordination number, we do not observe Zr−O bond breaking, i.e., exchange of the terminal, bound H_2O molecules with the bulk. Depending on the coordination, the monomer units take either a pentagonal bipyramid (seven-coordinated) or antiprism spatial arrangements (eight-coordinated), the latter also observed in the case of the tetramer.[47] The strain imposed by the binding pattern between the units induces different degrees of distortion in these geometries.

The monomers are bound by O-containing bridges, resulting in another repeating, and stable structural motif. For the dimer, we focus on the $Zr(OH)_2Zr$ unit, which also appears in the tetramer species. However, such a pattern does not hold the molecule together in the case of the studied linear trimer: the $Zr(OH)_2Zr(OH)_2Zr$ "backbone" of the trimer breaks into a dimer and a monomer unit within a very short time. A structure that seems to better accommodate the steric crowding present in the trimer involves a bridging O atom, which connects to all three Zr ions, and single OH or O bridges between each pair of Zr^{4+} ions. The $Zr(OH)_2Zr$

structural motif has a consistent geometry when the dimer and the tetramer are compared: the Zr−Zr distance is ∼3.8 Å and the Zr−O_{OH} distance is ∼2.2 Å. These distances are shorter and more dispersed in the thoroughly studied stacked trimer due to a much higher strain (3.5−3.6 Å Zr−Zr distance and 1.9−2.2 Å Zr−O_{OH} distance). Such a highly strained trimer geometry is the probable cause of the fluctuations of one of the monomer units.

As opposed to the tetramer, in which all the Zr ions are eight-coordinated, one of the dimer Zr ions is seven-coordinated. This lower coordination does not change in the course of the 10 ps simulation of the dimer in aqueous solution, i.e., a water molecule from the bulk does not fill the vacancy (such a process was observed in, e.g., aluminum chlorohydrate Al_{13} cluster, using the same simulation method and on a similar time scale[23]).

The present work indicates not only that the stacked trimer could exist but also that it may not be a very stable structure, due to a highly strained core consisting of three Zr ions connected by altogether four bridges, where one bridging oxygen atom is shared by all three Zr ions. We observed significant oscillations of one Zr monomer unit with respect to the other two in the first 50 ps of the gas-phase simulation. However, we were not able to detect a similar behavior in solution, due to the confinement of the trimer by the water formed cage around it. We suggest that this instability would be detected in solution as well, if a longer simulation was possible. This argument holds for a seemingly contradictory finding of an X-ray study of the Zr, Ti, and Hf binding to transferrin,[2] a protein that regularly binds iron, which suggests that the trinuclear cluster that is either grown within the protein or bound to the protein cleft is very similar to what we call the stacked trimer. The stability of the cluster within the cleft in this case might be enhanced by the confinement coming from the protein groups; without such confinement, the fluctuations of one of the Zr monomers would be possible.

V. Summary

Despite the importance and widespread use of zirconium hydroxy polynuclear clusters, certain important and basic aspects of their structure and dynamics are not known. This lack of information in some cases limits or even rules out our predictive power with respect to possible functions and applications as well as activities in known applications. By conducting a CPMD simulation study of the two smallest Zr^{4+} polynuclear species, we have provided the necessary basic information on their structure and dynamics in aqueous medium, in which most of the applications are conducted. Our study resulted in a detailed understanding of the structure, including repeating motifs, which will be used for studying larger Zr^{4+} polymers, such as the hexamer, and it reveals for the first time possible configurations of the dimer and trimer. Based on the observed fluctuating internal motion of one Zr monomer with respect to the other two, we postulate that the stacked trimer (structure obtained in our study) has a somewhat unstable structure and might persist only on a short time scale upon its formation, which might be the reason for conflicting experimental reports regarding its existence. Also, our study of the zirconium hexamer[55] reveals that it can be viewed as built from the trimer units. Thus, the trimer could be a transient species in the process of hexamer formation.

Acknowledgment. This research was supported in part by the Petroleum Research Fund administered by the American Chemical Society, in part by the Colgate-Palmolive Company. Computer time from Pittsburgh Supercomputing Center is greatly appreciated. N.R. and V.P. acknowledge support from the H. O. West Foundation and NSF (CHE-0420556) and thank Dr. Z. Liu and Dr. E. Birnbaum for helpful discussions.

References

(1) Ekberg, C.; Kallvenius, G.; Albinsson, Y.; Brown, P. L. *J. Solution Chem.* **2004**, *33*, 47−79.

(2) Alexeev, D.; Zhu, H. Z.; Guo, M. L.; Zhong, W. Q.; Hunter, D. J. B.; Yang, W. P.; Campopiano, D. J.; Sadler, P. J. *Nat. Struct. Biol.* **2003**, *10*, 297−302.

(3) Butler, A. *Nat. Struct. Biol.* **2003**, *10*, 240−241.

(4) Barondeau, D. P.; Getzoff, E. D. *Curr. Opin. Struct. Biol.* **2004**, *14*, 765−774.

(5) Rosenberg, A. H.; Fitzgerald, J. J. *Antiperspirants and Deodorants*; Marcel Dekker, Inc.: New York, Basel, 1999; pp 137−168.

(6) Northrup, C. J. M. J. Immobilization of U.S. defense nuclear wastes using the SYNROC process. In *Scientific Basis for Nuclear Waste Managment*; 1979; Vol. 2, p 265.

(7) Richens, D. T. *The Chemistry of Aqua Ions*; John Wiley & Sons: Chichester, New York, Weinheim, Brisbane, Singapore, Toronto, 1997; pp 207−220.

(8) Baes, C. F.; Mesmer, R. E. *The Hydrolysis of Cations*; John Wiley & Sons: New York, London, Sydney, Toronto, 1976.

(9) Car, R.; Parrinello, M. *Phys. Rev. Lett.* **1985**, *55*, 2471−2474.

(10) Pasquarello, A.; Petri, I.; Salmon, P. S.; Parisel, O.; Car, R.; Toth, E.; Powell, D. H.; Fischer, H. E.; Helm, L.; Merbach, A. E. *Science* **2001**, *291*, 856−859.

(11) White, J. A.; Schwegler, E.; Galli, G.; Gygi, F. *J. Chem. Phys.* **2000**, *113*, 4668−4673.

(12) Naor, M. M.; Van Nostrand, K.; Dellago, C. *Chem. Phys. Lett.* **2003**, *369*, 159−164.

(13) Lightstone, F. C.; Schwegler, E.; Allesch, M.; Gygi, F.; Galli, G. *Chem. Phys. Chem.* **2005**, *6*, 1745−1749.

(14) Lightstone, F. C.; Schwegler, E.; Hood, R. Q.; Gygi, F.; Galli, G. *Chem. Phys. Lett.* **2001**, *343*, 549−555.

(15) Amira, S.; Spangberg, D.; Zelin, V.; Probst, M.; Hermansson, K. *J. Phys. Chem. B.* **2005**, *109*, 14235−14242.

(16) Ikeda, T.; Hirata, M.; Kimura, T. *J. Chem. Phys.* **2005**, *122*, 024510.

(17) Ramaniah, L. M.; Bernasconi, M.; Parrinello, M. *J. Chem. Phys.* **1999**, *111*, 1587−1591.

(18) Ikeda, T.; Hirata, M.; Kimura, T. *J. Chem. Phys.* **2003**, *119*, 12386−12392.

(19) Lyubartsev, A. P.; Laasonen, K.; Laaksonen, A. *J. Chem. Phys.* **2001**, *114*, 3120−3126.

(20) Marx, D.; Sprik, M.; Parrinello, M. *Chem. Phys. Lett.* **1997**, *273*, 360−366.

(21) Rothlisberger, U.; Klein, M. L. *J. Am. Chem. Soc.* **1995**, *117*, 42−48.

(22) Pophristic, V.; Klein, M. L.; Holerca, M. N. *J. Phys. Chem. A* **2004**, *108*, 113−120.

(23) Pophristic, V.; Balagurusamy, V. S. K.; Klein, M. L. *Phys. Chem. Chem. Phys.* **2004**, *6*, 919−923.

(24) Sillanpaa, A. J.; Paivarinta, J. T.; Hotokka, M. J.; Rosenholm, J. B.; Laasonen, K. E. *J. Phys. Chem. A* **2001**, *105*, 10111−10122.

(25) Clearfield, A.; Vaughan, P. A. *Acta Crystallogr.* **1956**, *9*, 555−558.

(26) Muha, G. M.; Vaughan, P. A. *J. Chem. Phys.* **1960**, *33*, 194−199.

(27) Mak, T. C. W. *Can. J. Chem.* **1968**, *46*, 3491.

(28) Aberg, M. *Acta Chem. Scand. Ser. A - Phys. Inorg. Chem.* **1977**, *31*, 171−181.

(29) Zielen, A. J.; Connick, R. E. *J. Am. Chem. Soc.* **1956**, *78*, 5769.

(30) Johnson, J. S.; Kraus, K. A. *J. Am. Chem. Soc.* **1956**, *78*, 3937−3943.

(31) Angstadt, R. L.; Tyree, S. Y. *J. Inorg. Nucl. Chem.* **1962**, *24*, 913−917.

(32) Veyland, A.; Dupont, L.; Pierrard, J. C.; Rimbault, J.; Aplincourt, M. *Eur. J. Inorg. Chem.* **1998**, 1765−1770.

(33) Goedecker, S.; Teter, M.; Hutter, J. *Phys. Rev. B* **1996**, *54*, 1703−1710.

(34) Troullier, N.; Martins, J. L. *Phys. Rev. B* **1991**, *43*, 1993.

(35) Becke, A. D. *Phys. Rev. A* **1988**, *38*, 3098.

(36) Lee, C.; Yang, W.; Parr, R. G. *Phys. Rev. B* **1988**, *37*, 785.

(37) The solvation of Zr^{4+} ion will be addressed in a separate publication.

(38) Becke, A. D. *Phys. Rev. A* **1988**, *38*, 3098−3100.

(39) Lee, C. T.; Yang, W. T.; Parr, R. G. *Phys. Rev. B* **1988**, *37*, 785−789.

(40) Becke, A. D. *J. Chem. Phys.* **1993**, *98*, 1372.

(41) Hay, P. J.; Wadt, W. R. *J. Chem. Phys.* **1985**, *82*, 270−283.

(42) Frisch, M. J. T., G. W.; Schlegel, H. B.; Scuseria, G. E.; Robb, M. A.; Cheeseman, J. R.; Montgomery, J. A., Jr.; Vreven, T.; Kudin, K. N.; Burant, J. C.; Millam, J. M.; Iyengar, S. S.; Tomasi, J.; Barone, V.; Mennucci, B.; Cossi, M.; Scalmani, G.; Rega, N.; Petersson, G. A.; Nakatsuji, H.; Hada, M.; Ehara, M.; Toyota, K.; Fukuda, R.; Hasegawa, J.; Ishida, M.; Nakajima, T.; Honda, Y.; Kitao, O.; Nakai, H.; Klene, M.; Li, X.; Knox, J. E.; Hratchian, H. P.; Cross, J. B.; Bakken, V.; Adamo, C.; Jaramillo, J.; Gomperts, R.; Stratmann, R. E.; Yazyev, O.; Austin, A. J.; Cammi, R.; Pomelli, C.; Ochterski, J. W.; Ayala, P. Y.; Morokuma, K.; Voth, G. A.; Salvador, P.; Dannenberg, J. J.; Zakrzewski, V. G.; Dapprich, S.; Daniels, A. D.; Strain, M. C.; Farkas, O.; Malick, D. K.; Rabuck, A. D.; Raghavachari, K.; Foresman, J. B.; Ortiz, J. V.; Cui, Q.; Baboul, A. G.; Clifford, S.; Cioslowski, J.; Stefanov, B. B.; Liu, G.; Liashenko, A.; Piskorz, P.; Komaromi, I.; Martin, R. L.; Fox, D. J.; Keith, T.; Al-Laham, M. A.; Peng, C. Y.; Nanayakkara, A.; Challacombe, M.; Gill, P. M. W.; Johnson, B.; Chen, W.; Wong, M. W.; Gonzalez, C.; Pople, J. A. *Gaussian03*; Gaussian, Inc.: Wallingford, CT, 2004.

(43) Martyna, G. J.; Klein, M. L.; Tuckerman, M. *J. Chem. Phys.* **1992**, *97*, 2635−2643.

(44) Nose, S. *J. Chem Phys.* **1984**, *81*, 511.

(45) Nose, S. *Mol. Phys.* **1984**, *52*, 255.

(46) Hoover, W. G. *Phys. Rev. A* **1985**, *31*, 1695.

(47) Rao, N.; Holerca, M. N.; Klein, M. L.; Pophristic, V. *J. Phys. Chem. A* **2007**, *111*, 11395−11399.

(48) Safonov, A. A.; Bagatur'yants, A. A.; Korkin, A. A. *Microelectron. Eng.* **2003**, *69*, 629−632.

(49) Zhao, X.; Ceresoli, D.; Vanderbilt, D. *Phys. Rev. B* **2005**, *71*, 085107.

(50) Foschini, C. R.; Filho, O. T.; Juiz, S. A.; Souza, A. G.; Oliveira, J. B. L.; Longo, E.; Leite, E. R.; Paskocimas, C. A.; Varela, J. A. *J. Mater. Sci.* **2004**, *39*, 1935−1941.

(51) Chen, S. G.; Yin, Y. S.; Wang, D. P. *J. Mol. Struct.* **2004**, *690*, 181−187.

(52) Zhong, W.; Parkinson, J. A.; Parsons, S.; Oswald, I. D. H.; Coxall, R. A.; Sadler, P. *J. Inorg. Chem.* **2004**, *43*, 3561−3572.

(53) Rose, J.; Bruin, T. J. M. D.; Chauveteau, G.; Tabary, R.; Hazemann, J. L.; Proux, O.; Omari, A.; Toulhoat, H.; Bottero, J. Y. *J. Phys. Chem. B* **2003**, *107*, 2910−2920.

(54) Saukkoriipi, j.; Sillanpaa, A.; Laasonen, K. *Phys. Chem. Chem. Phys.* **2005**, *7*, 3785.

(55) Rao, N.; Pophristic, V. To be published.

(56) Zielen, A. J.; Connick, R. E. *J. Am. Chem. Soc.* **1956**, *78*, 5785−5792.

(57) Tribalat, S.; Schriver, L. *Bulletin De La Societe Chimique De France Partie I-Physicochimie Des Systemes Liquides Electrochimie Catalyse Genie Chimique*; 1975; pp 2012−2014.

CT7001094